International Journal of Phytoremediation

ISSN: 1522-6514 (Print) 1549-7879 (Online) Journal homepage: http://www.tandfonline.com/loi/bijp20

Phosphorus sorption capacity of biochars from different waste woods and bamboo

Yingxue Li, Defu Xu, Yidong Guan, Kewei Yu & Wenhua Wang

To cite this article: Yingxue Li, Defu Xu, Yidong Guan, Kewei Yu & Wenhua Wang (2019): Phosphorus sorption capacity of biochars from different waste woods and bamboo, International Journal of Phytoremediation, DOI: 10.1080/15226514.2018.1488806

To link to this article: https://doi.org/10.1080/15226514.2018.1488806

Published online: 18 Jan 2019.

INTERNATIONAL JOURNAL OF PHYTOREMEDIATION
https://doi.org/10.1080/15226514.2018.1488806

Phosphorus sorption capacity of biochars from different waste woods and bamboo

Yingxue Li[a], Defu Xu[b,c], Yidong Guan[b], Kewei Yu[d], and Wenhua Wang[e]

[a]School of Applied Meteorology, Nanjing, China; [b]Collaborative Innovation Center of Atmospheric Environment and Equipment Technology, Nanjing, China; [c]Jiangsu Key Laboratory of Atmospheric Environment Monitoring and Pollution Control, Nanjing, China; [d]Department of Biological and Environmental Sciences, Troy University, Troy, AL, USA; [e]Guizhou Institute of Soil and Fertilizer, GAAS, Guiyang, China

ABSTRACT

Four biochars were made via pyrolysis at 500 °C using different waste plant materials, including tree branches from *Cinnamonum campora* (L.) Pres (CCP), *Eriobotrya japonica* (Thunb.) Lindl (EJL), *Rohdea roth* (RR) and bamboo shoots (*Phyllostachys sulphurea*) (PS). Phosphorus sorption capacities of the biochars were studied by isothermal experiments on their sorption kinetics. Results show that P sorption to the three wood biochars (CCP, EJL, and RR) fitted well with Lagergren pseudo second order model. However, P release was found in the PS biochar and sand amended with the PS biochar treatments during the isothermal sorption experiment. Phosphorus sorption capacity of the CCP biochar, EJL biochar and RR biochar was 4,762.0, 2, 439.0 and 1, 639.3 mg/kg, respectively. The CCP biochar showed the highest P sorption capacity due to its higher pH, lower dissolved P content, larger surface area (23.067 m^2/g) and pore volume (0.058 cm^3/g). The PS biochar showed the lowest P sorption due to its higher dissolved P content, more carboxyl groups, and smaller surface area (2.982 m^2/g) and pore volume (0.017 cm^3/g). Results suggest that the CCP biochar could be a potential alternative adsorbent for P sorption, such as removing P in wastewater treatment by constructed wetlands.

KEYWORDS

Biochar; constructed wetland; phosphorus; sorption

Introduction

Biochar can be produced from thermochemical decomposition of biomass in an oxygen limited environment (Lehmann 2007; Manya 2012), which has highly aromatic carbon structure, resulting in resistance in decomposition (Keiluweit et al. 2010). Biochars can be used as adsorbents for purifying wastewater, pathogens and gases (Wang et al. 2015). In addition, biochars can be added into soils to improve soil structure (Cox et al. 2012; Jha 2010).

Constructed wetlands (CW) are of technologies used for purifying wastewater, which have many favorable characteristics such as low construction cost, low operation cost, and simple management (Kadlec and Wallace 2008). High removal efficiency of biochemical oxygen demand (BOD) in wastewater was reported in CW (De Rozari et al. 2015). However, removal efficiency of phosphorus (P) in wastewater varied (Ayaz et al. 2012), depending on different substrates. Various materials have been used as a substrate to improve P removal in CW. Three types of materials could be used as substrates in CW: (1) natural materials including sands, gravels and soil; (2) man-made products such as clay and alunite; (3) by-products such as fly ash and slag (Vohla et al. 2011). Different substrates may have different P removal efficiencies. The efficiency of P removal in a CW with sand was reported to decrease after operation for a few months (Arias et al. 2001). However, sand amended with red mud was reported to be effective in P removal from secondary effluent (Lucas and Greenway 2010). Therefore, selecting a suitable substrate could be an effective approach to enhance P removal.

Biochars have been used for wastewater treatment. Compared to an activated carbon obtained from coconut, a better P removal was found in a biochar from digested sugar beet tailing (Yao et al. 2011). Up to 50% manure P could be absorbed by a hardwood biochar produced via slow pyrolysis (Sarkhot et al. 2013). Similarly, P sorption capacity was reported as 79% and 76% for a biochar obtained from corn stover (*Zea mays* L.) and from switchgrass (*Panicum virgatum* L.), respectively (Chintala et al. 2014). These findings suggest that biochars could be a potential alternative substrate for CW to enhance P removal from wastewater.

Biochars can affect the availability and retention of P, in which pH plays an important role. Some studies showed that biochars were able to enhance available P in soils (Zhang et al. 2016). The findings can be interpreted by following reasons: (1) Biochars can increase soil alkalinity (Biederman and Harpole 2013) and subsequently alters P interactions with metals (such as Al^{3+}, Fe^{3+}, and Ca^{2+}) (Wang et al. 2012); (2) Biochars can delay P sorption or

CONTACT Defu Xu defuxu1@163.com Collaborative Innovation Center of Atmospheric Environment and Equipment Technology, Nanjing, China.
Color versions of one or more of the figures in the article can be found online at www.tandfonline.com/bijp.

precipitation in soils because of their direct adsorption with the soil metals; (3) Biochars may enhance P availability by direct release of soluble P (Atkinson et al. 2010). However in other reports, decreased P availability was found when soils were amended with biochars. For example, biochar application significantly increased P retention in soils and consequently decreased P levels in leachate solutions (Novak et al. 2009), due to its common properties of higher ash content, cation exchange capacity (CEC), larger surface area and porosity. Borchard et al. (2012) confirmed that biochars with higher ash contents had higher P sorption capacities in their study. Laird et al. (2010) showed that biochar with larger surface area and porosity would enable them to adsorb more P. Therefore, previous reports on P retention and availability in biochars were inconsistent, and the results depended on the soil conditions and origin of biochar.

Biochar is an effective, low-cost and eco-friendly soil ameliorant, and has ability to immobilize toxic elements (Malińska et al. 2017). Biochar may stimulate plant growth, result in higher leaf number, and increase plant total biomass (Trupiano et al. 2017). Ihuoma et al. (2018) demonstrated that addition of biochar to soil resulted in increased aboveground (shoot) biomass. The coconut husk biochar had a positive impact on maize growth, especially the aboveground biomass (Maria et al. 2018). Plants play an important role in CW, and their growth can benefit from biochar addition. At present, biochars have been used in CW to purify wastewater (Li et al. 2017). However, the effect of biochar on removing P in CW can vary. For example, Gupta et al. (2015) revealed that P removal efficiency was higher with biochar obtained from woody materials of oak tree (*Quercus sp*) than with gravels in a horizontal subsurface flow CW. However, De Rozari et al. (2016) showed that P removal efficiency in a subsurface CW was better with pure sand media than with sand amended with biochar. Therefore, limited and controversial information exits on the effect of biochar on P removal in CW. The objectives of this study were to investigate P sorption capacity of different biochars and biochar-amended sand, and to investigate the effects of biochar characteristics on P sorption capacity.

Materials and methods

Materials

Four plant materials were obtained from the campus in Nanjing University of Information Science and Technology, Nanjing, China, including branches of *Cinnamonum campora (L.) Pres* tree (CCP), *Eriobotrya japonica (Thunb.) Lindl* tree (EJL), *Rohdea Roth* (RR) tree, and bamboo (*Phyllostachys sulphurea*) (PS). Three wood biochars and one bamboo biochar were made by washing the plant materials with distilled water, and then putting the air-dried samples in a ceramic pot for pyrolysis in a muffle furnace under N_2 atmosphere. The pyrolyzing temperature in the muffle furnace was raised to 500 °C at a rate of 5 °C/min, and kept at the peak temperature for 2 h, and then cooled to room temperature. All biochars were passed through 2.0 mm sieve after grinding using a stainless grinding machine. A river sand sample was obtained from the local market, and its particle size distribution is listed in Table 1.

Table 1. Particle size distribution of sand.

Size	(% w/w)[a]				
	0−0.3 mm	0.3−1.0 mm	1.0−2.0 mm	2.0−3.0mm	3.0−5.0 mm
Sand	32	26	7	10	25

[a]w-weight of size fraction as a percentage of total weight of sample.

Batch sorption experiment

Two-gram biochar samples were placed in a 50-mL centrifuge tube and suspended in 20 mL of 0.01 M KCl solution containing 100, 200, 300, 400, and 500 mg P/L KH_2PO_4. In addition, sand-biochar mixes were prepared to investigate the effect of biochar on P sorption in sand. The PS biochar was added at rates of 0, 5, 10, 15 and 20% by volume to make various sand-PS biochars. Two-gram sand-PS biochar mixtures were placed in a 50-mL centrifuge tube and suspended in 20 ml of 0.01 M KCl solution containing 10, 20, 40, 60, and 80 mg P/L KH_2PO_4. All measurements were repeated three times. Microbial growth was inhibited by adding two drops of chloroform to the samples. The centrifuge tubes were shaken in a reciprocal shaker at 25 °C with 200 rpm after sealing their lids. After 24 h, the samples were centrifuged at 4,000 rpm for 10 min, and the supernatant was filtered through a 0.45-μm filter before analyzing the P content.

Sorption kinetics experiment

Kinetics of P sorption in the biochars were studied at 25 °C, and the initial pH for each solution was adjusted to 7. Two-gram biochars were added to centrifuge tubes with 50 mg P/L. The mixtures were shaken at 200 rpm in a mechanical shaker with 10-mL aliquot taken at 30 min, 1, 4, 8, 12 and 24 h, respectively, from each sample. All samples were filtered and analyzed for P content.

Analysis methods

A mixture with 1:2.5 (w/v) substrate/water was prepared for determining pH values of the biochars and sand using a pH meter (PHS-3C, Rex acidity meter). After equilibrating for 1 h, dissolved P content of the biochars and sand in a 1:60 (w/v) substrate/water mixture was analyzed by method of Murphy and Riley (1962). Major procedure includes: (1) combine 0.2 mL sample, 3.8 mL distilled water, and 1 mL Murphy and Riley reagent, (2) mix thoroughly and allow reacting for 10-20 min, and (3) determine P concentration at a wavelength of 700 nm using a UV-VIS spectrophotometer (UV5200).

Infrared (IR) spectra of the biochars were measured using 2 mg grounded sample in a KBr pellet on a FTIR by scanning from 4,000 to 400 reciprocal centimeters (Thermo Fisher Nicolet iS5), averaging 10 scans at 1 cm^{-1} interval with a resolution of 4 cm^{-1}. Scanning electron microscope

Table 2. pH and dissolved P of the studied biochars.

Sample	pH	Dissolved P (mg/L)
CCP biochar	11.06 ± 0.62 a	0.33 ± 0.014 fg
EJL Biochar	10.33 ± 0.30 ab	0.48 ± 0.028 ef
RR biochar	9.78 ± 0.76 bc	0.72 ± 0.028 de
PS biochar	9.65 ± 0.58 bc	3.69 ± 0.269 a
Sand	7.45 ± 0.14 d	0.05 ± 0.014 g
Sand +5% PS biochar	8.85 ± 0.59 c	0.70 ± 0.071de
Sand +10% PS biochar	9.12 ± 0.07 c	0.89 ± 0.113 cd
Sand +15% PS biochar	9.27 ± 0.21 c	1.10 ± 0.141 bc
Sand +20% PS biochar	9.45 ± 0.07 bc	1.29 ± 0.184 b

CCP, EJL, RR and PS represented *Cinnamonum campora (L.)Pres*, *Eriobotrya japonica (Thunb.) Lindl*, *Rohdea Roth* and *Phyllostachys sulphurea*, respectively. SE, standard error. Data are means ± SE of $n = 3$. Different letters in the same column indicate significant differences in different biochars or sand amended biochar ($p < 0.05$).

(SEM) imaging analysis (Hitachi SU1510) was conducted to compare the structure and surface characteristics of the biochars. Zeta potential was determined by a Zeta potentiometer (Zetasizer Nano ZS90). The specific surface area and porosity properties of the biochars were measured by N_2 adsorption isotherms at 77 K with the Brunauer–Emmett–Teller (BET) method using an Automated Gas Sorption Analyzer (Autosorb-iQ-MP, Quantachrome, USA)

The amount of P sorption to each biochar was calculated according to following equations:

$$Qe = \frac{(C_0 - C_e)V}{W} \quad (1)$$

$$Qt = \frac{(C_0 - C_t)V}{W} \quad (2)$$

where Q_e is the mass of adsorbed at equilibrium (mg/g), Q_t (mg/g) is the adsorbed amount of P per unit weight of adsorbent at the given time. C_0 and C_t (mg/L) are the aqueous sorbate P concentrations at initial and time t, respectively. C_e is equilibrium aqueous P concentration (mg/L). V is the volume of the aqueous solution (L), and W (g) is the mass of the adsorbent.

The Langmuir isotherm equation is shown as:

$$Qe = \frac{(C_L - C_m)V}{(1 + K_L C_e)} \quad (3)$$

where K_L and Q_m is the Langmuir constant and the maximum sorption capacity (mg/g), respectively.

The Freundlich isotherm is expressed as:

$$Qe = K_F C_e^{\frac{1}{n}} \quad (4)$$

where K_F and 1/n represents the Freundlich constant (mg/kg) and heterogeneity factor, respectively.

The kinetics of P sorption in biochars were described using a pseudo first order kinetic model (5), a pseudo second order kinetic model (6) and an intra-particle diffusion model (7).

$$Q_t = Q_e(1 - e^{-k_1 t}) \quad (5)$$

$$Qt = \frac{k_2 Q_e^2 t}{1 + k_2 Q_e t} \quad (6)$$

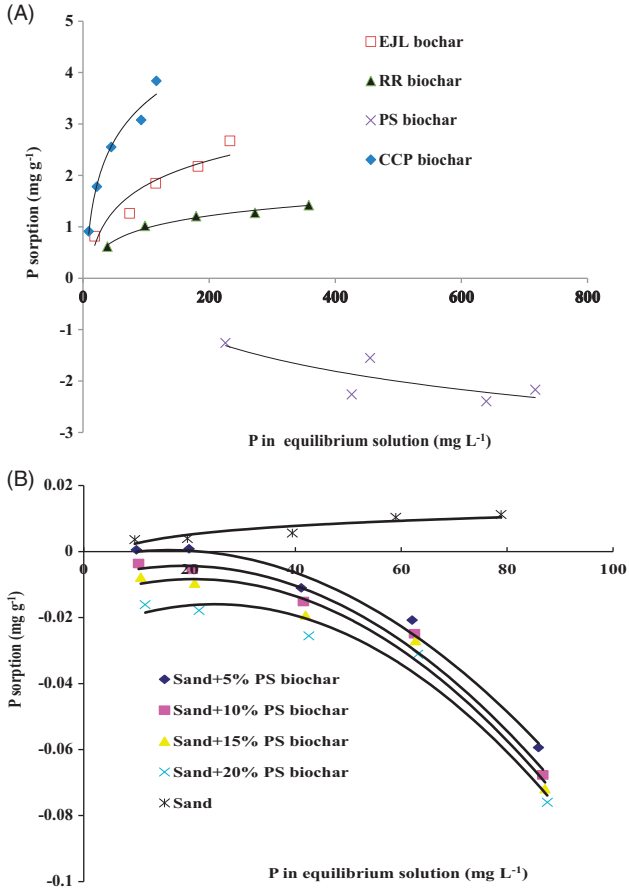

Figure 1. Phosphorus sorption or desorption isotherms for different biochars (A), and mixtures of biochar and sand (B). CCP, EJL, RR and PS represent *Cinnamonum campora (L.) Pres, Eriobotrya japonica (Thunb.) Lindl, Rohdea Roth* and *Phyllostachys sulphurea*, respectively.

Table 3. Langmuir, Freundlich isotherm parameters for phosphorus sorption onto three wood biochars and sand.

	Langmuir model			Freundlich model		
Biochar	Q_m(mg/kg)	K_L(L/g)	R^2	k_F(mg/kg)	1/n	R^2
CCP biochar	4,762.0	0.126	0.997	0.399	0.363	0.9701
EJL biochar	2,439.0	0.063	0.911	0.372	0.463	0.9645
RR biochar	1,639.3	0.025	0.996	0.253	0.527	0.9521
sand	10.582	0.047	0.761	0.829	0.581	0.880

CCP, EJL and RR represented *Cinnamonum campora (L.)Pres, Eriobotrya japonica (Thunb.) Lindl*, and *Rohdea Roth*, respectively.

$$Q_t = k_i t^{1/2} + C \quad (7)$$

where k_1, k_2 and k_i represents the rate constant of the pseudo first order sorption (min^{-1}), the pseudo second order (kg mg^{-1} min^{-1}), and the intra-particle diffusion (mg kg^{-1} $min^{-0.5}$), respectively.

Statistical analysis

Statistical analysis was performed using SPSS 12.0. A one-way analysis of variance (ANOVA) was conducted for biochar characteristics. In this analysis, surface area, pore volume, average pore diameter, pH and dissolved P were dependent variables, respectively, and biochars or sand amended biochar were independent variables. Tukey test

was performed to detect the statistical significance of differences ($p < 0.05$) between means of treatments.

Results and discussion

Initial characteristics of the biochars

Dissolved P and pH values of the studied biochars are shown in Table 2. Among the four biochars, the CCP biochar showed the highest pH, and the PS biochar presented the lowest pH value. The PS biochar showed much higher dissolved P content than all the wood biochars. Among the three wood biochars, CCP biochar had the lowest dissolved P content. When adding the PS biochar into sand, both the pH and dissolved P content of the sand-PS biochar mixtures were increased proportionally. In summary, the CCP, EJL and RR biochar made from wood showed higher pH and lower dissolved P than the PS biochar.

Phosphorus sorption

Phosphorus sorption curves of the four biochars and mixtures of sand-biochar are shown in Figure 1. The amount of P sorption to the three wood biochars increased with the initial P concentration (Figure 1A). Taken CCP biochar for example, when the initial P concentration was 100 mg/L and 500 mg/L, the amount of P sorption was 0.91 mg/g and 3.84 mg/g, respectively. Result was similar to that of Lăcrămioara and Laura (2016), who reported that capacity of heavy metal sorption by mustard waste biomass increased with the initial heavy metal concentration. The amount of P sorption to sand was also increased when the initial P concentration increased (Figure 1B). However, P release from the PS biochar occurred during the whole sorption isotherms (Figure 1A), and the amount of released P was higher when increasing the portions of biochar to sand (Figure 1B). This result is in line with the results obtained by Bradley et al. (2015) who reported that the total leaching P increased when sand amended with higher portion of biochar from poplar (*Populus maximowiczii*).

The Langmuir and Freundlics isotherm parameters of different samples are shown in Table 3. According to R^2 value, the experimental data fitted to the Langmuir and Freundlich models. As shown in Table 3, the CCP biochar had the highest P Langmuir sorption maximum (4,762.0 mg/kg), and the RR biochar showed the lowest (1, 639.3 mg/kg). As shown in Table 3, for the three wood biochars, the bonding energy (K_L) followed the order of CCP > EJL > RR. Compared to the three wood biochars, P sorption maximum of the sand was the lowest (Table 3). In addition, the K_F value of CCP biochar was greater than those of other biochars, such as K_F values of CCP and RR biochar were 0.399 and 0.253, respectively, which means that the P sorption capacity of the CCP biochar was larger than those of all other biochars due to stronger interaction between the P and CCP biochar.

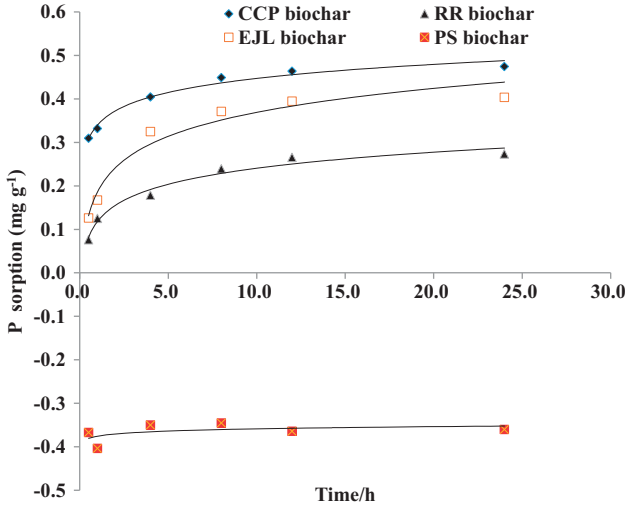

Figure 2. Phosphorus kinetic sorption curves of four biochars. CCP, EJL, RR and PS represent *Cinnamonum campora (L.) Pres, Eriobotrya japonica (Thunb.) Lindl, Rohdea Roth* and *Phyllostachys sulphurea*, respectively.

Phosphorus sorption kinetics

Phosphorus sorption kinetics of the four biochars are shown in Figure 2. Phosphorus release from the PS biochar occurred during the entire experimental period. However, the amount of P sorption to the three wood biochars increased over time. During the kinetic process, P sorption to the three wood biochars was quickly reached an equilibrium after 12 h of contact time (Figure 2).

The sorption data were used to fit with different kinetic models to investigate P sorption, and to determine kinetic parameters from the three sorption models. The results (Table 4) show that the pseudo-second order model consistently presented a better fit compared to the intra-particle diffusion model. Limousin et al. (2007) and Wang et al. (2011) also demonstrated that many metals and heavy elements follow this pattern. Among the different biochars, the pseudo second order rate constants (K_2) for the RR biochar and EJL biochar (3.4×10^{-5} and 3.1×10^{-5}) were lower than that of the CCP biochar (6.8×10^{-5}). These results indicate that the pseudo second order model can be used to predict the kinetic process of P sorption to biochars. In this study, the average R^2 value of the three wood biochars for the intra-particle diffusion model was 0.963. These results were similar to those of Takaya et al. (2016), who believed that both rapid surface sorption of P and slower intra-particle diffusion through the adsorbent occurred simultaneously.

Effect of characteristics of biochar on P sorption capacity

According to Table 2 and Table 3, the CCP biochar with the highest P sorption maximum could be related to the highest pH. The results were similar to those of Xu et al. (2014), who found that P sorption was increased when soil pH was increased in savanna soils. However, P sorption to the biochars decreased with the increase of dissolved P, which contributed to P release from the biochars themselves. The

Table 4. Kinetic parameters of phosphorus sorption onto three wood biochars obtained from different sorption models.

	Pesudo first order		Pesudo second order		Intra-particle diffusion	
Sample	K(min^{-1})	R^2	k_2(g μg^{-1} min^{-1})	R^2	Kp(μg g^{-1} $min^{-0.5}$)	R^2
CCP biochar	4.0×10^{-3}	0.9994	6.8×10^{-5}	0.9996	7.479	0.9753
EJL biochar	4.9×10^{-3}	0.9942	3.1×10^{-5}	0.9995	13.028	0.9366
RR biochar	4.5×10^{-3}	0.9782	3.4×10^{-5}	0.9970	8.5247	0.9774

CCP, EJL and RR represented *Cinnamonum campora (L.) Pres, Eriobotrya japonica (Thunb.) Lindl* and *Rohdea Roth*, respectively.

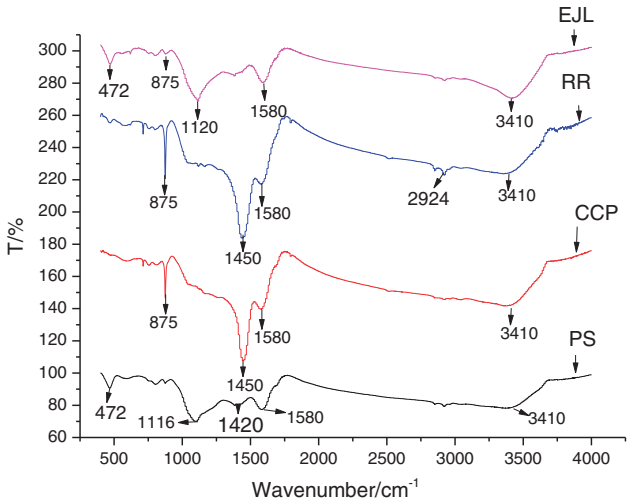

Figure 3. IR spectra of different biochars. CCP, EJL, RR and PS represent *Cinnamonum campora (L.) Pres, Eriobotrya japonica (Thunb.) Lindl, Rohdea Roth* and *Phyllostachys sulphurea*, respectively.

Table 5. Physical and chemical properties of the studied biochars

Sample	CCP	EJL	RR	PS
Surface area (m^2/g)	23.067 ± b	119.953 ± a	1.935 ± c	2.982 ± c
Pore volume (cm^3/g)	0.058 ± b	0.095 ± a	0.030 ± c	0.017 ± d
Average pore diameter (nm)	41.841 ± a	3.810 ± c	42.272 ± a	27.225 ± b
Zeta potential (mV)	20.5 ± 0.71c	25.6 ± 3.68bc	30.1 ± 1.27b	39.5 ± 2.12a

CCP, EJL, RR and PS represented *Cinnamonum campora (L.)Pres, Eriobotrya japonica (Thunb.) Lindl, Rohdea Roth* and *Phyllostachys sulphurea*, respectively. SE, standard error. Data are means ± SE of $n = 3$. Different letters in the same line indicate significant differences in different biochars ($p < 0.05$).

exchangeable Ca could significantly affect P sorption because of Ca precipitation or co-sorption with the added P (Agbenin 1995). Elsa et al. (2018) showed that P removal process by biochar was mainly due to chemical bonding or chemisorption involving sharing electrons between phosphate ionic species and Ca-doped biochar as described by the Equation (8). High concentration of Ca^{2+} and high pH of the solution are fundamentals for precipitation as brushite.

$$Ca^{2+} + HPO_4^{2-} + 2H_2O \rightarrow CaHPO_4.2H_2O_{(s)} \quad (8)$$

Murphy and Stevens (2010) demonstrated that biochar application increased Ca concentration in soil solutions, which could increase P sorption. Xu et al. (2014) also demonstrated that an increase in P sorption was related to the increase in exchangeable Ca after biochar application to soil. In this study, compared to sand, P sorption capacities of the three wood biochars were all higher, which could be related to the Ca exchange of the biochars and higher pH (Table 2).

The IR spectra of the four biochars are shown in Figure 3. The adsorption bands from 472 cm^{-1} for EJL and RS biochar was symmetrical stretching vibration of Si-O. All three wood biochars had a 875 cm^{-1} band, which was attributed to aromatic C-H out of plane bending that indicated a greater degree of aromaticity. The absorption bands from 2,924 cm^{-1} for RR biochar was asymmetric C–H stretching vibrations of methyl groups (Lăcrămioara and Laura, 2016). The band at 3,410 cm^{-1} was attributed to stretching vibration of N-H. The band at 14,200 cm^{-1} of the PS biochar represented the antisymmetric and symmetric C = O (C–O) stretching vibration of carboxyl groups. The band at 1,116 cm^{-1} of PS biochar was assigned to C–O–C stretching vibration in the aliphatic ethers, which represented oxygenated functional groups of lignin. Kloss et al. (2012) demonstrated that carboxyl groups contributed to negative surface charges. De Rozari et al. (2016) showed that carboxyl groups on the biochar surface could result in repulsion of negatively charged ions like phosphate. As shown in Table 5, zeta potential of the PS biochar was lowest among the tested biochars. Therefore, P release from the PS biochar could be related to the more negative surface charges.

The SEM images of the studied biochars are shown in Figure 4. Among the four biochars, the CCP biochar showed more and uniform hollow channels. Compared to the CCP biochar, the EJL biochar had bigger pore size with relatively lower porosity (Figure 4). The RR biochar had different diameters of hollow channel. The PS biochar showed lower porosity compared with the EJL and CCP biochar. These structures may be important for a large internal surface area and a high sorption ability of a biochar as an excellent absorbent.

The specific surface area, pore volume and average pore diameter varied significantly for the studied biochars (Table 5). These were similar to a report by Unai et al. (2016), who demonstrated that acid treatment at 0.2 mmol acid g^{-1} precursor increased BET area by about 80%, compared to untreated bone char. The EJL biochar showed the largest BET surface areas (119.953 m^2/g), and the RR biochar showed the lowest BET surface areas (1.935 m^2/g). Average pore diameter of the biochars was in an order as: RR (42.272 nm) and CCP (41.841 nm) > PS (27.225 nm) > EJL (3.810 nm). The results indicate that the EJL biochar presented the largest BET surface areas than the other biochars, but its average pore diameter was the smallest. Cui et al. (2016) showed that *Z. caduciflora* biochar had a larger surface area (84.05 m^2/g) than those of *C. indica* biochar, *P. purpureum Schum* biochar, *T. dealbata* biochar, *P. australis* biochar and *V. zizanioides* biochar; The *Z. caduciflora* biochar with the smallest pore size indicated that abundant

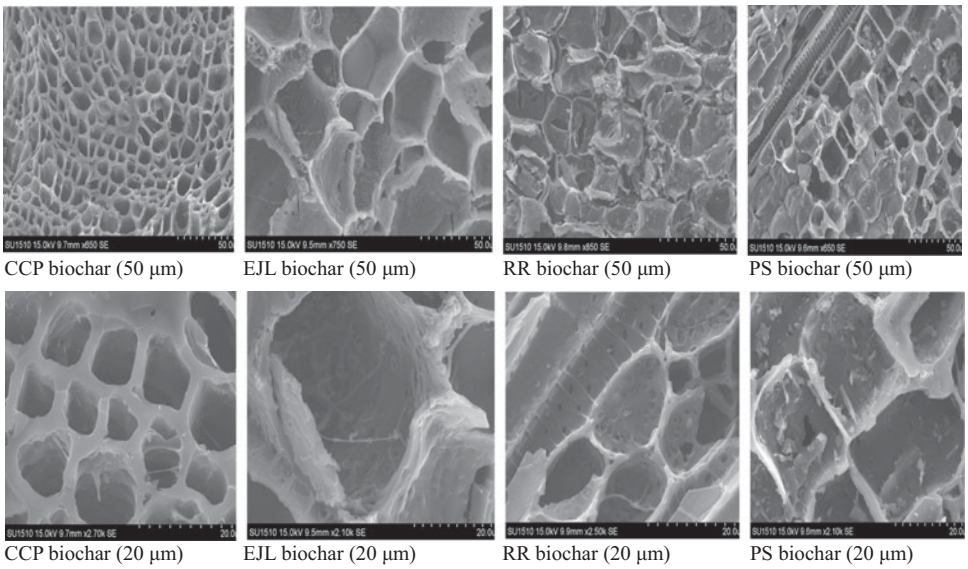

Figure 4. SEM images of the biochars. CCP, EJL, RR and PS represent *Cinnamonum campora (L.) Pres, Eriobotrya japonica (Thunb.) Lindl, Rohdea Roth* and *Phyllostachys sulphurea*, respectively.

micropores mostly contributed to the largest surface area. Therefore, in this study, the EJL biochar with a larger surface area than the other biochars was due to its abundant micropores. Pore volume of the biochars followed the order of EJL ($0.095\,cm^3/g$) > CCP ($0.058\,cm^3/g$) > RR ($0.03\,cm^3/g$) > PS ($0.017\,cm^3/g$). The PS biochar showed the lowest P sorption, due to its lowest pore volume (Table 5). The CCP and EJL biochar presented higher P sorption, due to their larger surface area and pore volume. Compared to the P sorption to the CCP biochar, the EJL biochar showed the lowest average pore diameter, resulted in lower P sorption (Table 5). Biochars with larger BET surface areas and average pore diameter are beneficial for P sorption.

Conclusion

The P sorption maximum was 4,762.0 mg/kg, 2,439.0 mg/kg, 1,639.3 mg/kg respectively for the CCP biochar, EJL biochar and RR biochar. The CCP biochar showed the highest P sorption maximum, due to its higher pH and lower dissolved P. Phosphorus release from the PS biochar occurred during the entire sorption experiment, due to its higher dissolved P and lower pH. In addition, the lower P sorption capacity of the PS biochar could be related to the carboxyl groups that would lead to repulsion of negatively charged ions like phosphate. The SEM images showed that the pore characteristic was different for the different biochars. The higher P sorption capacity of the CCP biochar was related to the larger BET surface areas and average pore diameter. From this study, it is concluded that the CCP biochar could be a potential alternative substrate for P sorption with various applications, such as wastewater treatment in CW.

Funding

This work was supported by the Natural Science Foundation of Jiangsu Province (Grants No BK20141477), National Natural Science Foundation of China (Grant No. 40901257), Scientific Research Foundation for the Returned Overseas Chinese Scholars, and a project funded by the Priority Academic Program Development of Jiangsu Higher Education Institutions.

References

Agbenin JO. 1995. Phosphorus sorption by three cultivated savanna Alfisols as influenced by pH. Nutr Cycl Agroecosyst. 44:107–112.

Arias C, Del Bubba M, Brix H. 2001. Phosphorus removal by sands for use as media in subsurface flow constructed reed beds. Water Res. 35:1159–1168.

Atkinson CJ, Fitzgerald JD, Hipps NA. 2010. Potential mechanisms for achieving agricultural benefits from biochar application to temperate soils: a review. Plant soil. 337(1):1–18.

Ayaz SÇ, Aktas Ö, Findik N, Akca L. 2012. Phosphorus removal and effect of adsorbent type in a constructed wetland system. Desalin Water Treat. 37:152–159.

Biederman LA, Harpole WS. 2013. Biochar and its effects on plant productivity and nutrient cycling: a meta-analysis. GCB Bioenergy 5:202–214.

Borchard N, Wolf A, Laabs V, Aeckersberg R, Scherer H, Moellerand A, Amelung W. 2012. Physical activation of biochar and its meaning for soil fertility and nutrient leaching a greenhouse experiment. Soil Use Manag. 28:177–184.

Bradley A, Larson R, Runge T. 2015. Effect of wood biochar in manure-applied sand columns on leachate quality. J Environ Qual. 44:1720–1728.

Chintala R, Schumacher TE, McDonald LM, Clay DE, Malo DD, Papiernik SK, Clay SA, Julson JL. 2014. Phosphorus sorption and availability from biochars and soil/biochar mixtures. Clean-Soil Air Water. 42:626–634.

Cox J, Downie A, Jerkins A, Hickey M, Lines-Kelly R, McClintock A, Powell J, Singh BP, Zwieten LV. 2012. Biochar in Horticulture: Prospects for the Use of Biochar in Australian Horticulture. NSW Trade and Investment, Australia.

Cui XQ, Hao HL, Zhang CK, He ZL, Yang XE. 2016. Capacity and mechanisms of ammonium and cadmium sorption on different wetland-plant derived biochars. Sci Total Environ. 539:566–575.

De Rozari P, Greenway M, Hanandeh A El. 2015. An investigation into the effectiveness of sand media amended with biochar to remove BOD_5, suspended solids and coliforms using wetland mesocosms. Water Sci Technol. 71:1536–1544.

De Rozari P, Greenway M, Hanandeh A El. 2016. Phosphorus removal from secondary sewage and septage using sand media amended with biochar in constructed wetland mesocosms. Sci Total Environ. 569-570:123–133.

Elsa A, Mohan J, Graham B, Phil S. 2018. Isotherms, kinetics and mechanism analysis of phosphorus recovery from aqueous solution by calcium-rich biochar produced from biosolids via microwave pyrolysis. J Environ Chem Eng. 6:395–403.

Gupta P, Ann TW, Lee SM. 2015. Use of biochar to enhance constructed wetland performance in wastewater reclamation. Environ Eng Res. 21:36–44.

Ihuoma NA, Moses N A, Amos M O, John D C, Okoro N, Emmanuel BC. 2018. Influence of biochar aged in acidic soil on ecosystem engineers and two tropical agricultural plants. Ecotox Environ Safe. 153:116–126.

Jha P. 2010. Biochar in agriculture-prospects and related implications. Curr Sci. 99:12–18.

Kadlec RH, Wallace S. 2008. Treatment wetlands. Boca Raton: CRC press.

Keiluweit M, Nico PS, Johnson MG, Kleber M. 2010. Dynamic molecular structure of plant biomass-derived black carbon (Biochar). Environ Sci Technol. 44:1247–1253.

Kloss S, Zehetner F, Dellantonio A, Hamid R, Ottner F, Liedtke V, Schwanninger M, Gerzabek MH, Soja G. 2012. Characterization of slow pyrolysis biochars: effects of feedstocks and pyrolysis temperature on biochar properties. J Environ Qual. 41:990–1000.

Lăcrămioara N, Laura B. 2016. Optimization of process parameters for heavy metals biosorption onto mustard waste biomass. Open Chemistry 14: 175–187.

Laird D, Fleming P, Wang BQ, Horton R, Karlen D. 2010. Biochar impact on nutrient leaching from a Midwestern agricultural soil. Geoderma 158:436–442.

Lehmann J. 2007. A handful of carbon. Nature 447:143–144.

Li M, Wu HM, Zhang J, Ngo HH, Guo WS, Kong Q. 2017. Nitrogen removal and nitrous oxide emission in surface flow constructed wetlands for treating sewage treatment plant effluent: Effect of C/N ratios. Bioresour Technol. 240:157–164.

Limousin G, Gaudet JP, Charlet L, Szenknect S, Barthes V, Krimissa M. 2007. Sorption isotherms: a review on physical bases, modeling and measurement. Appl Geochem. 22:249–275.

Lucas WC, Greenway M. 2010. Phosphorus retention by bioretention mesocosms using media formulated for phosphorus sorption: response to accelerated loads. J Irrig Drain Eng. 137:144–153.

Malińska K, Golańska M, Caceres R, A Rorat, P Weisser. 2017. Biochar amendment for integrated composting and vermicomposting of sewage sludge-the effect of biochar on the activity of *Eisenia fetida* and the obtained vermicompost. Bioresour Technol. 225:206–214.

Manya JJ. 2012. Pyrolysis for biochar purposes: a review to establish current knowledge gaps and research needs. Environ Sci Eng. 46:7939–7954.

Maria G, Cheryl M, Andre QA, Kairon RA. 2018. Positive and negative effects of biochar from coconut husks, orange bagasse and pine wood chips on maize (*Zea mays* L.) growth and nutrition. Catena 162:414–420.

Murphy J, Riley JP. 1962. A modified single solution method for the determination of phosphate in natural waters. Analyt Chim Acta. 27:31–36.

Murphy PNC, Stevens RJ. 2010. Lime and gypsum as source measures to decrease phosphorus loss from soils to water. Water Air Soil Pollut. 212:101–111.

Novak JM, Busscher WJ, Laird DL, Ahmedna M, Watts DW, Niandou MAS. 2009. Impact of biochar amendment on fertility of a southeastern coastal plain soil. Soil Sci. 174:105–112.

Sarkhot D, Ghezzehei T, Berhe A. 2013. Effectiveness of biochar for sorption of ammonium and phosphate from dairy effluent. J Environ Qual. 42:1545–1554.

Takaya CA, Fletcher LA, Singh S, Anyikude KU, Ross AB. 2016. Phosphate and ammonium sorption capacity of biochar and hydrochar from different wastes. Chemosphere 145:518–527.

Trupiano D, Cocozza C, Baronti S, Amendola C, Vaccari FP, Lustrato G, Lonardo SD, Fantasma F, Tognetti R, Scippa GS. 2017. The effects of biochar and its combination with compost on lettuce (Lactuca sativa l.) growth, soil properties, and soil microbial activity and abundance. International J. Agro. 2:1–12.

Unai I-V, Irene S, Lorena Z, Jose LA. 2016. Preparation of a porous biochar from the acid activation of pork bones. Food Bioprod Process. 98:341–353.

Vohla C, Koiv M, Bavor HJ, Chazarenc F, Mander Ü. 2011. Filter materials for phosphorus removal from wastewater in treatment wetlands-a review. Ecol Eng. 37:70–89.

Wang T, Arbestain MC, Hedley M, Bishop P. 2012. Predicting phosphorus bioavailability from high-ash biochars. Plant soil. 357:173–187.

Wang Z, Guo H, Shen F, Yang G, Zhang Y, Zeng Y, Wang L, Xiao H, Deng S. 2015. Biochar produced from oak sawdust by lanthanum (La)-involved pyrolysis for sorption of ammonium (NH_4^+), nitrate (NO_3^-), and phosphate (PO_4^{3+}). Chemosphere 119:646–653.

Wang Z, Liu G, Zheng H, Li F, Ngo HH, Guo W, Liu C, Chen L, Xing B. 2015.Investigating the mechanisms of biochar's removal of lead from solution. Bioresour Technol. 177:308–317.

Wang Z, Nie E, Li J, Yang M, Zhao Y, Luo X, Zheng Z. 2011. Equilibrium and kinetics of sorption of phosphate onto iron-doped activated carbon. Environ Sci Pollut Res Int. 19:2908–2917.

Xu G, Sun JN, Shao HB, Scott XC. 2014. Biochar had effects on phosphorus sorption and desorption in three soils with differing acidity. Ecol Eng. 62:54–60.

Yao Y, Gao B, Inyang M, Zimmerman AR, Cao X, Pullammanappallil P, Yang L. 2011. Biochar derived from anaerobically digested sugar beet tailings: characterization and phosphate removal potential. Bioresour Technol. 102:6273–6278.

Zhang HZ, Chen CR, Evan MG, Sue EB, Yang H, Zhang DK. 2016. Roles of biochar in improving phosphorus availability in soils: a phosphate adsorbent and a source of available phosphorus. Geoderma 276:1–6.